International Journal for Housing Science and Its Applications
Publish August 4, 2025. Volume 46, Issue 3 Pages 2010-2022

https://doi.org/10.70517/ijhsa463159

Calculation Method of New Energy Consumption Capacity Considering Main Grid Currents and Section Constraints

Ding Li[1,*], Yalu Sun[1], Yanpeng Ma[1], Dezhen Kong[1] and Shenglei Du[1]
[1] State Grid Gansu Economic Research Institute, Lanzhou, Gansu, 730050, China
Corresponding authors: (e-mail: 425430718@qq.com).

Abstract New energy generation technology has the prospect of large-scale development and commercialization, so it is of great significance to study the new energy consumption capacity of regional power grids, and to promote the planning of regional power grids to be compatible with new energy development. In this paper, considering various constraints, the optimal current calculation model is constructed, and the traditional time series production simulation is used to simulate the new energy consumption capacity of the system during the cycle. We introduce the associated cross-section limit calculation to reduce the risk of new energy abandonment and at the same time take into account the consumption capacity, and establish a linear tidal current-based calculation and new energy associated cross-section limit power optimization model. Simulation experiments are designed to evaluate the new energy consumption. Considering the new energy under the section constraints, the new energy output in the sending section increases continuously from 07:00 to 10:00, and the peak value reaches 2,452MW, meanwhile, the thermal power output in the section is automatically suppressed, and the section control is more delicate, which can greatly improve the utilization rate of the section. After simulation through the power system operation, it is found that there is a certain degree of wind abandonment in each scheme, among which the P2 scheme has the smallest wind abandonment, and the overall wind abandonment is 9217.195 MW•h, which is significantly smaller than the other schemes.

Index Terms optimal tidal current calculation, traditional time series production, correlation section limit, power abandonment risk, new energy consumption capacity

I. Introduction

With the increasing environmental awareness of people, the installed capacity of new energy power generation in China has grown significantly, in which the proportion of renewable energy sources such as wind and solar energy in the power system has been increasing year by year, becoming a key part of the energy structure [1]-[3]. Due to the volatility and randomness of new energy generation such as wind and solar energy, this leads to differences in the output curves of new energy generation, making it difficult to supply power generation stably [4], [5]. The power system is accomplished simultaneously in generation, supply, and consumption, which requires real-time dynamic balance between power generation, transmission, distribution, and consumption within the system [6], [7]. If the output of new energy power generation is unstable, the real-time balancing demand at this time is difficult to meet, which brings serious challenges to the stable operation of the power grid and the security of power supply [8]. In order to cope with large-scale and variable new energy access scenarios, a variety of automatic assessment methods for new energy consumption capacity combined with automated assessment techniques have emerged. Huang, S. et al. analyzed the historical loads and renewable energy outputs of the regional power system to obtain load curves and new energy output curves, and combined with the grid aggregation model to explore the limits of its new energy consumption capacity, which provides a reference for power planning in the region [9]. Meng, X. et al. proposed to use the energy storage absorption curve as a planning index to measure the new energy consumption capacity, by visualizing the relationship between the energy storage capacity and the amount of electrical energy absorption, and establishing a capacity matching model with the goal of cost minimization, in this regard, optimizing the peaking rate and adjusting the proportion of new energy installations, to achieve the maximization of the new energy utilization rate and the balance between supply and demand [10]. Huang, K. et al. introduced the time series production simulation theory to simulate the power absorption capacity and production capacity of PV distribution network, which can accurately calculate the consumption capacity of PV distribution network, and then provide data support for the planning and construction of power system [11]. Shi, Q. et al. designed an active distribution network type identification method based on source-load matching to quantify the source-load operation data of regional distribution networks based on relevant indexes, which is highly practical in

active distribution network planning for new energy power systems [12]. Gils, H. C. et al. constructed the Renewable Energy Mix (REMix) energy system model and applied it to the task of evaluating the capacity expansion and hourly scheduling of photovoltaic and wind power systems capable of balancing the energy supply of the power system at minimum cost [13]. However, the above method fails to take into account the tidal current constraints, resulting in the power flow in the transmission grid cannot be accurately controlled and is prone to overload or voltage runaway. Based on this, it is possible to automatically simulate the time-sequence production process of the transmission grid by introducing the tidal current constraints of the transmission grid and the idea of automatic selection of the tidal current of the key time section in order to provide a more accurate and reliable basis for the planning of new energy development of the power grid [14]-[16].

In this paper, the new energy data information in the power grid is processed through the current calculation, and the optimal current calculation method is used to analyze the new energy consumption capacity. The traditional time series production simulation method is used to simulate the new energy consumption of the system during the cycle, the corresponding objective function is set, and the linear tidal current is added as a constraint to the model, so as to construct a time series production simulation model based on the linearized tidal current constraint. The concept of risk is introduced to constitute the associated section limit power calculation model to solve the safety and stability problems in the process of new energy consumption. The main network current and cross-section constraint formulas are linked to establish a new energy consumption associated cross-section limit power optimization model based on the linearized current calculation. Through system simulation experiments, the new energy consumption capacity assessment model is verified, and the model is applied to a regional power grid to assess the new energy consumption in the region.

II. Calculation of new energy consumption capacity taking into account main network currents and cross-section constraints

II. A.Ideas for calculating new energy consumption

II. A. 1) Calculation of 66kV consumption calculation capacity calculation idea

Firstly, this paper analyzes the calculation idea of DG consumption capacity, and calculates the peak margin of the grid with the boundary condition of the planning level year or the typical daily maximum load of the grid, and considers that the peak margin is the installed capacity that can accept wind power and photovoltaic power supply, so as to calculate the space for new energy consumption; secondly, it builds a trend calculation model, and analyzes the current status quo grid (e.g., transformer substation, line) conditions whether it meets the distributed power supply access, and finally gives suggestions for upgrading the new energy consumption. Finally, it gives the current grid transformation suggestions to enhance the new energy consumption.

II. A. 2) Calculation of 10kV consumption capacity

In this paper, various constraints should be considered comprehensively in the establishment of the assessment model, so that its network framework and new energy consumption capacity can be optimized, and the calculation method of optimal trend is used to analyze the new energy consumption capacity [17].

The idea is as follows: by setting the installed access capacity of wind power and photovoltaic, the objective function is the maximum value of the actual output of the new energy unit, to establish a new energy maximum consumption model of a regional power grid, taking into account the limitations of the climbing rate of its conventional unit, grid size, multi-scenario calculation, can be considered to use the DC model calculation. The general form of the model is:

$$\max(C_w P_w^t + C_{pv} P_{pvi}^t) \tag{1}$$

$$P_{Gi}^i + P_{wi}^i + P_{pvi}^i + P_i^i = P_{Li}^i \tag{2}$$

$$P_{Gi,\min} \le P_{Gi}^i \le P_{Gi,\max} \tag{3}$$

$$-r_G^D \cdot \Delta t \le P_{Gi}^t - P_{Gi}^{t-1} \le U_{Gi} \cdot \Delta t \tag{4}$$

$$P_{i-j} \le P_{i-j,\max} \tag{5}$$

$$t = 1, 2, \cdots, 24 \tag{6}$$

Eq. (1) is the objective function to maximize the output of wind turbines and photovoltaic and consider its generation cost, Eq. (2) is the nodal power balance equation, Eq. (3) is the upper and lower constraints on the output of conventional units, Eq. (4) is the constraints on the unit creep, Eq. (5) is the constraints on the line tidal

currents, and Eq. (6) is the time series [18]. The above model solution, using a certain time series (24 time periods / day), the new energy power generation output is equal to its actual output, for the new energy all consumption, if the output is less than the actual output, there is a discarded light, wind phenomenon.

The voltage overrun deviation range is selected as $U_{\min} = -3\%U_N$, $U_{\max} = 7\%U_N$.

Conventional unit output upper and lower limits constraints: $P_{\min} = XPU_n, P_{\max} = PU_a$, X takes the value of the lower limit of the thermal 600,000-unit operating mode as 40% (national average), the lower limit of the 300,000-unit operating mode as 48% (national average), and the heating units operate unit capacity The lower limits are 60% during normal operation (national average) and 80% during winter heating (to meet the basic needs of electric equipment and heating), respectively.

Transformer transmission capacity constraint: $P_\alpha \le P_{TN}$ Line transmission capacity constraint: $P_L \le P_{LN}$. Network-wide power flow constraint: $N-1$. Consider 220kV substation delivering power without backfeeding.

Power balance: take the maximum moment of a typical day in summer.

II. B. Considering the new energy consumption capacity of the main network trend

II. B. 1) Treatment of new energy sources in tidal current calculations

The trend calculation of distribution network is the main means and measures for power system analysis, and it is also an important content in the planning study of distribution network, through the trend calculation, it can be a more comprehensive mastery of the basic grid information such as current, voltage, network loss, active, reactive, etc., which is of great significance for the new energy development and planning in distribution network.

Considering that new energy is generally installed in the terminal of the power supply network to realize the purpose of new energy local consumption. New energy grid-connected nodes in the electrical distance with the load node is very close, while taking into account the new energy to maximize the use of the problem, such as photovoltaic power plants generally control the output of photovoltaic arrays in the maximum power point, so this paper considers the new energy node as a negative value of the PQ node.

Figure 1 shows the new energy system wiring, as the new energy is generally accessed at the end of the distribution network, it will have an impact on the distribution network current and other conditions. When the new energy is connected to the load node at the end of the line, since the new energy can meet the user's demand for electricity to a certain extent, it can effectively reduce the power transmitted through the transmission network, making the stable operation limit at the end of the line (B point) increase, thus improving the load capacity of the line. Since new energy sources are intermittent, if they are set in the middle of the line they must undergo substation capacity expansion, as well as load capacity expansion of the transmission corridor. Therefore, these transmission capacity constraints are important factors limiting the installed capacity of new energy sources.

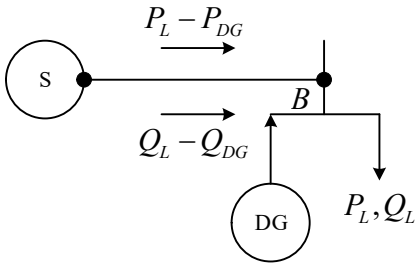

Figure 1: Wiring diagram of the new energy system

II. B. 2) Current Calculation Methods for Distribution Networks Containing New Energy Sources

In this paper, the forward back generation method is used to calculate the tidal currents of the distribution network, and the calculation relationship between the nodes is shown below:

$$P_i = P_{i-1} - R_{i-1}(P_{i-1}^2 + Q_{i-1}^2)/U_{i-1}^2 - P_{Lj} + P_{DGi} \tag{7}$$

$$Q_i = Q_{i-1} - X_{i-1}(P_{i-1}^2 + Q_{i-1}^2)/U_{i-1}^2 - Q_{Li} + Q_{DGi} \tag{8}$$

$$U_i^2 = U_{i-1}^2 - 2(P_{i-1}R_{i-1} + Q_{i-1}X_{i-1}) + (R_{i-1}^2 + X_{i-1}^2)(P_{i-1}^2 + Q_{i-1}^2)/U_{i-1}^2 \tag{9}$$

where P_i is the active power of node i, Q_i is the reactive power of the node, U_i is the voltage of the node, $R_i - 1, X_i - 1$ are the resistance and reactance of the node $i-1$, $i = 1,2,\cdots,n$, and n is the node of line Total number.

(1) Wind turbine current calculation

Since the asynchronous motor needs to absorb reactive power from the power system when it is connected to the grid, which is different compared with the synchronous generator set, the steady state calculation model of the asynchronous wind turbine is shown in Fig. 2.

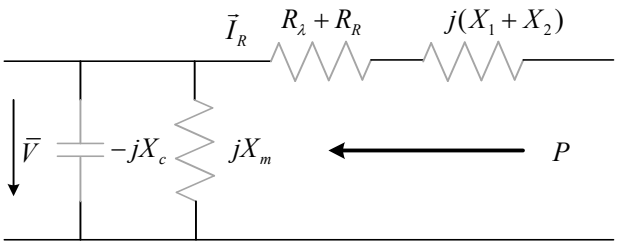

Figure 2: Steady-state model of asynchronous wind motor

According to the model shown in Fig. 2, the reactive power can be expressed according to the power equation relationship as:

$$Q = V^2 \frac{X_c - X_m}{X_c X_m} + X \frac{V^2 + 2RP}{2(R^2 + X^2)} - X \frac{\sqrt{(V^2 + 2RP)^2 - 4P^2(R^2 + X^2)}}{2(R^2 + X^2)} \tag{10}$$

where V represents the system voltage, X_c and X_m denote the capacitance parameter and the excitation reactance, respectively, X denotes the sum of the leakage reactances of the stator and rotor of the asynchronous machine, and P represents the active power.

A simplified model of Eq. (11) can be obtained by following the McLaughlin polynomials and neglecting the effect of the asynchronous machine resistance R:

$$Q = V^2 \frac{X_c - X_m}{X_c X_m} + \frac{PX}{V^2} \tag{11}$$

The steps for calculating the tidal current at a given wind speed are:

1) Find the active power P_w of the wind farm, and then calculate the reactive power $Q^{(0)}$ absorbed by the wind farm at $V_i^{(0)}$.

2) Perform the tidal current calculation, using the newly obtained, recalculate the reactive power $Q_m^{(k+1)}$, and iterate repeatedly until the end of the calculation.

(2) Current calculation of PV unit

Since the PV unit and doubly-fed asynchronous unit can realize the decoupling control of active and reactive power, it can be equated to a PQ node, and this paper adopts the constant power model.

II. C. Calculation model of new energy consumption capacity

II. C. 1) Objective function

In order to maximize the new energy consumption of the new energy power system, the traditional time series production simulation takes the maximum new energy consumption of the system in the simulation cycle as the objective function:

$$\max \sum_{i=1}^{r} (P_i^W + P_i^{PV}) \tag{12}$$

where T is the production simulation period, P_i^W is the sum of the power generated by each wind farm at t moment that is consumed by the system, and P_t^{PV} is the sum of the power generated by each photovoltaic (PV) farm at t moment that is consumed by the system.

II. C. 2) Constraints

(1) Standby capacity constraints:

$$\sum_{u=1}^{N_a} P_{u,t}^{G,\max} \mu_{u,t} - \sum_{u=1}^{N_a} P_{u,t}^{G} \geq P_{re} \tag{13}$$

$$\sum_{u=1}^{N_a} P_{u,t}^{G} - \sum_{u=1}^{N_a} P_{u,t}^{G,\min} \mu_{u,t} \geq N_{re} \tag{14}$$

where $P_{u,t}^{G.\max}, P_{u,t}^{G.\min}$ are the upper and lower limits of thermal unit u output respectively, $P_{u,t}^{G}$ is the thermal unit u output, $\mu_{u,t}$ is the thermal unit u operation state, is a Boolean variable, 0 means the unit is in the shutdown state, 1 indicates that the unit is in operation, P_{re}, N_{re} are the required positive and negative rotating standby capacity of the system, respectively.

(2) Thermal power unit output constraint:

$$P_{u,t}^{G.\min} \mu_{u,t} \leq P_{u,t}^{G.\max} \leq P_{u,t}^{G.\max} \mu_{u,t} \tag{15}$$

(3) Thermal unit creep constraints:

$$P_{u,t}^{G} - P_{u,t-1}^{G} \leq P_{u,t}^{G.U} \mu_{u,t-1} + (1-\mu_{u,t-1}) P_{i}^{G.\min} \tag{16}$$

$$P_{u,t-1}^{G} - P_{u,t}^{G} \leq P_{u}^{G,D} \mu_{u,t} + (1-\mu_{u,t}) P_{u,t}^{G,\min} \tag{17}$$

where $P_{u,t}^{G.U}, P_{u,t}^{G.D}$ are the upward and downward climbing capacity of thermal power unit u, respectively.

(4) Thermal power unit operation state constraints:

$$\mu_{u,t} - \mu_{u,t-1} = \mu_{u,t}^{SU} - \mu_{u,t}^{SD} \tag{18}$$

$$0 \leq \mu_{u,t}^{SU} + \mu_{u,t}^{SD} \leq 1 \tag{19}$$

where $\mu_{u,t}^{SU}$ is the startup state of unit u, a Boolean variable, 0 means not in startup state, 1 means in startup state, and $\mu_{u.t}^{SD}$ is the shutdown state of unit u, a Boolean variable, 0 means not in shutdown state, 1 means in shutdown state.

(5) Minimum start/stop time constraint for thermal power units:

$$T_u^{on} \mu_{u,t}^{SU} \leq \sum_{h=t}^{t+T_u^{on}-1} \mu_{u,t} \forall t \leq T - T_u^{on} + 1 \tag{20}$$

$$T_u^{off} \mu_{u,t}^{SD} \leq \sum_{h=t}^{t+T_u^{on}-1} (1-\mu_{u,t}) \forall t \leq T - T_u^{off} + 1 \tag{21}$$

(6) New energy output constraints.

$$0 \leq P_{\omega,t}^{W} \leq P_{\omega,t}^{W,\max} \tag{22}$$

$$0 \leq P_{z,t}^{PV} \leq P_{z,t}^{PV,\max} \tag{23}$$

where $P_{\omega,t}^{PV,\max}, P_{z,t}^{PV,\max}$ are the maximum output power of wind turbine generator ω, z at t moment, respectively.

The linear tidal current is added as a constraint into the traditional time-series production simulation model to construct a time-series production simulation model based on the linearized tidal current constraint:

$$P(i,t) = \sum^{u\in\Omega^G} P_{u,t}^{G} + \sum^{w\in\Omega^w} P_{u,t}^{W} + \sum^{z\in\Omega^{PV}} P_{z,t}^{PV} - P_{i,t}^{load} \tag{24}$$

$$Q(i,t) = \sum^{s\in\Omega^G} Q_{i,t}^{G} - Q_{i,t}^{D} \tag{25}$$

$$P(i,t) = g_{ii} \frac{2V_{i,t}^{k} + k - 2}{k} + \sum_{j\neq i}^{N_{i-1}} \left(g_{ij} \frac{V_{i,t}^{k} - V_{j,t}^{k}}{k} - b_{ij} \theta_{ij,t} \right) \tag{26}$$

$$Q(i,t) = -b_i \frac{2V_{i,t}^k + k - 2}{k} + \sum_{\substack{j=1 \\ j \neq i}}^{N_{-1}} \left(-b_{ij} \frac{V_{i,t}^k - V_{j,t}^k}{k} - g_{ij}\theta_{ij,t} \right) \tag{27}$$

$$P_{ij}^{L.\min} \leq g_{ij} \frac{V_{i.t}^k - V_{j.t}^k}{k} - b_{ij}\theta_{ij.t} \leq P_{ij}^{L.\max} \tag{28}$$

$$V_i^{\min} \leq V_{i.t} \leq V_i^{\max} \tag{29}$$

$$\theta_i^{\min} \leq \theta_{i.t} \leq \theta_i^{\max} \tag{30}$$

where $V_i^{\max}$ and $V_i^{\min}$ are the upper and lower limits of the voltage amplitude of node i, $\theta_i^{\max}$ and $\theta_i^{\min}$ are the upper and lower limits of the voltage amplitude of node i, respectively.

II. D. Calculation of Limits of Associated Sections

II. D. 1) Associated sections

The correlation cross section mentioned refers to a set of transmission cross sections in which the limit powers exist coupled to each other. The topological relationship of associated sections in the actual power grid can be simply summarized into three categories, and the related cross-section schematic is shown in Fig. 3. For example, the series-type correlation cross-section formed by the main grid of Northwest Grid and Xinjiang interconnection channel (Xinjiang outgoing cross-section, Dunyu cross-section, Gaoyu cross-section, etc.), and the series/parallel hybrid correlation cross-section formed by Southwest, Central, and North China (Chuanyu cross-section, Chongqing-Erongo cross-section, EHV Changnan line, etc.).

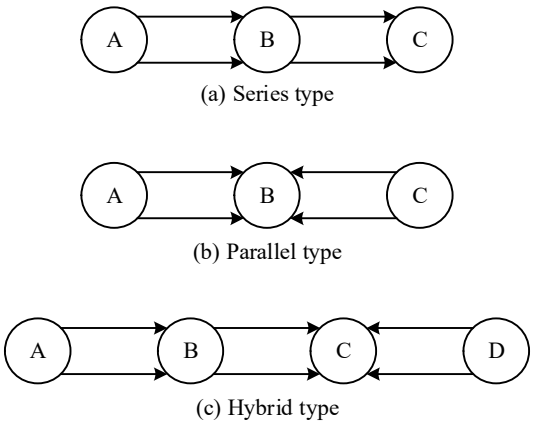

Figure 3: Schematic diagram of the associated section

The online calculation of associated cross-section limit power mainly provides cross-section limits for intra-day spot trading, intra-day and real-time dispatch planning. Existing methods are generally based on the conservative principle of safety and stability, with the goal of maximizing the sum of the associated cross-section limit power. For the high proportion of new energy power grids with greatly increased uncertainty factors, it is easy to have a mismatch between the cross-section limit and the actual new energy power generation capacity, resulting in wind and light abandonment, and restricting the grid's new energy consumption capacity. In order to meet the demand for coordinated optimization of multi-section transmission capacity and new energy consumption capacity of high proportion new energy power grids, this paper introduces the concept of risk and improves the existing method from two perspectives: 1) The minimization of the risk of curtailment of renewable energy is one of the goals of coordinated optimization, and the overall transmission capacity of the power grid is improved, while taking into account the capacity of new energy consumption, and 2) the boundary conditions corresponding to the ultimate power are changed from the deterministic "safety and stability margin" to the "safety and stability risk" considering the uncertainty, and the problem of relatively conservative and poor economy of traditional methods is solved by controlling the risk within an acceptable range.

II. D. 2) Optimization models

Specifically, the correlation section limit power optimization model established in this paper taking into account new energy consumption is shown in Eqs. (31) and (32):

$$F = \max\left[\sum_{i=1}^{N}(\lambda_i P_{\lim,i}) - \lambda_R f_R(P_{\lim,i})\right] \tag{31}$$

$$f_E(P_{\lim,i}) \le \alpha_{\max} \tag{32}$$

where: N is the number of associated sections, $P_{\lim,i}$ is the section i-limit power (i.e., section limit), $\lambda_i \in [0,1]$ is the weight coefficient of section i-limit power, f_R is the new energy power abandonment risk function of the system, λ_R is the weight coefficient of the risk term, f_E is the system security and stability risk function, and $\alpha_{\max}$ is the maximum value of security and stability risk that the system can accept.

A few notes on the model:

(1) The value of λ_i is closely related to the topological relationship of the associated section and the location of the load center. Assuming that the load center is located in area C, and the main optimization objective is set as the maximum power receiving capacity of area C, the weight coefficients $\lambda_{BC}, \lambda_{DC}$ of section B→C and section D→C should be taken as (0, 1], and λ_{AB} should be taken as 0.

(2) The new energy power abandonment risk mainly considers the wind and light abandonment risk, and the risk size depends on the section limit power, power abandonment probability and power abandonment, which can be obtained by probabilistic trend calculation and statistical analysis based on the predicted power interval and probability of each new energy field station.

(3) The security and stability risk mainly considers the new energy off-grid risk, generation and load loss risk, and the risk size depends on the section limit power, fault probability and consequences (including the amount of new energy off-grid, generation and load loss, etc.). Among them, the consequences of the fault need to consider the second and third line of defense action of the grid, which is calculated by post-fault time domain simulation.

III. Calculation of new energy consumption capacity for typical cases

III. A. Introduction to the algorithm

III. A. 1) Load levels

In order to validate the established new energy consumption capacity assessment model, the improved IEEE30 node test system is utilized for simulation and analysis, and the electrical parameters of each node and branch circuit are obtained from the MATPOWER trend calculation software package case30.m file. The system consists of six thermal generating units with climbing rates set at 25% of the rated capacity per hour of regulation, and one hydroelectric generating unit with an installed capacity of 100 MW, which is set in the output range of 0 ~ 100% and connected to 26 nodes. A wind farm with a total installed capacity of 500 MW is connected to 19 nodes. A photovoltaic power plant with a total installed capacity of 300 MW is connected to 17 nodes. The electrochemical energy storage system configured in this paper adopts the most commonly used lithium iron phosphate battery, access to 15 nodes. Setting ω_L and ω_{WV} to 0.08 and 0.06 respectively, the branch power limit is set to 200 MW. Load, wind and PV data are simulated by using the historical data of Xinjiang region in 2022 [19].

The 2022 load curve of the region is shown in Fig. 4, and the simulation time step is 1h, and the sequence of load output presents fluctuation in the range of 1050MW~1610MW in the time period of 0-9000h.

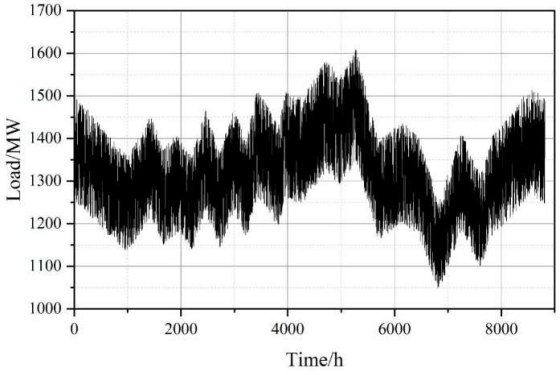

Figure 4: Load output sequence of the region in 2022

III. A. 2) Wind and PV output levels

The normalized wind and PV power outputs are shown in Fig. 5, Fig. (a) shows the normalized wind power output series in 2022, and Fig. (b) shows the PV power output time series. The wind power output sequence mainly fluctuates between 0.4 and 0.8, and the wind power output decreases to about 0.5 after 8000h. The PV power output sequence mainly fluctuates between 0.2 and 1.05, with eight peaks, which occur at 500, 1500, 2500, 3500, 5000, 6000, 7500, and 8500h, respectively.

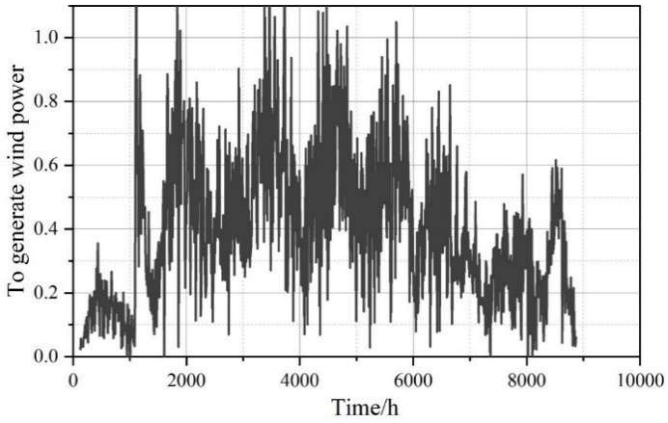

(a)Normalized wind power output sequence in 2022

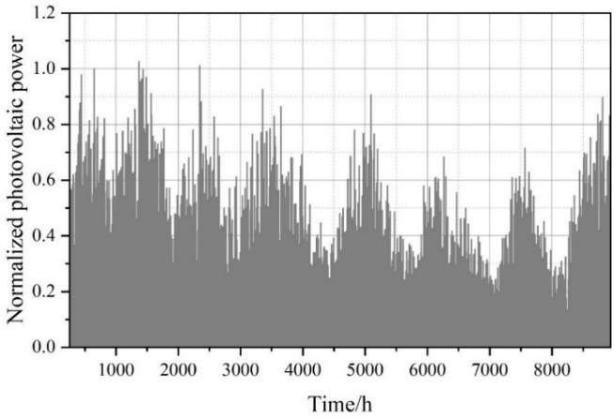

(b)Normalized PV output sequence in 2022

Figure 5: The wind power and the light power are normalized

III. B. Model solving

According to the above basic parameter data, in this section, the time series production simulation is carried out for January-December respectively, and the example solving environment is a laptop computer with 16 GB of memory, Intel Core i7 CPU and 2. 20 GHz main frequency, and Matlab platform is used to call CPLEX solver to optimize the solving of the model established in this paper. The consumption of wind power and photovoltaic in each month is shown in Fig. 6, Fig. (a) shows the wind power consumption and Fig. (b) shows the photovoltaic consumption. It can clearly reflect the amount of abandoned power, the amount of consumption and the abandonment rate of wind power and PV in each month.

The results show that the total annual wind power consumption is 1523076.923MWh, the total abandoned power of wind power is 120678.733MWh, the abandoned power rate of wind power is 6.776%, and the utilization hours of wind power generation is 3042.312h. The abandoned power rate of wind power is larger in February, March, and October, which is above 10%. The total annual PV consumption was 5517259.615MWh, the total PV power abandonment was 51965.498MWh, the PV power abandonment rate was 8.934%, and the number of PV power generation utilization hours was 1,742.621h. The PV power abandonment rate was larger in May, September and October, all above 12%.

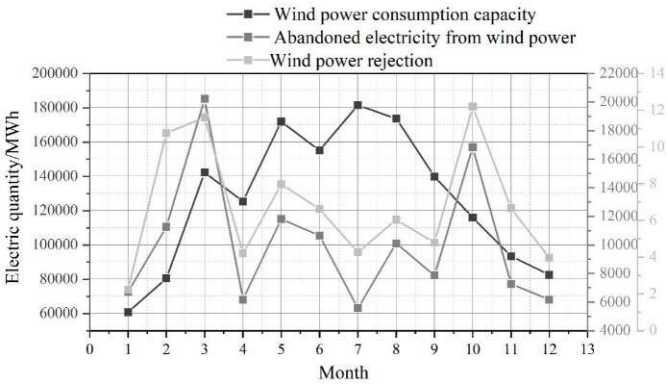

(a)Wind power rejection situation

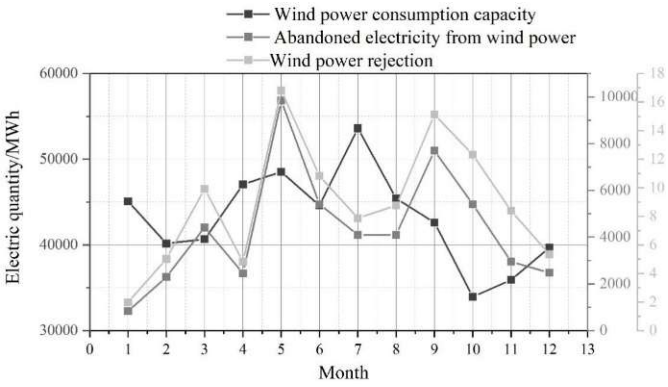

(b)PV information

Figure 6: The situation of the wind power and the various months of the light

III. C. New Energy Consumption Results Considering Cross Section Constraints

III. C. 1) Analysis of new energy consumption results based on cross-section constraints

By applying the optimization model proposed in this paper to the local grid, the thermal power and new energy output curves and section operation trend curves are shown in Fig. 7, and the change curves of the allowable cut-off in the sending section in the same time period are shown in Fig. 8.

The new energy output curve and section operation trend are shown in Fig. 7, and the new energy output curve and section operation trend are shown in Fig. 8. In the time period of 07:00-10:00, the new energy output in the outgoing section continues to increase, and the peak value reaches 2,452MW, while at the same time, the thermal power output in the section is automatically suppressed. With the further increase of new energy output, the load factor of the section rises to full load, and thermal power is suppressed to the minimum (around 2500MW). In the 09:00-16:00 time period (midday when the new energy output is large), the actual operating trend of the sending section is close to the stability limit, with fewer burrs, and the section control is finer, which can greatly improve the utilization rate of the section.

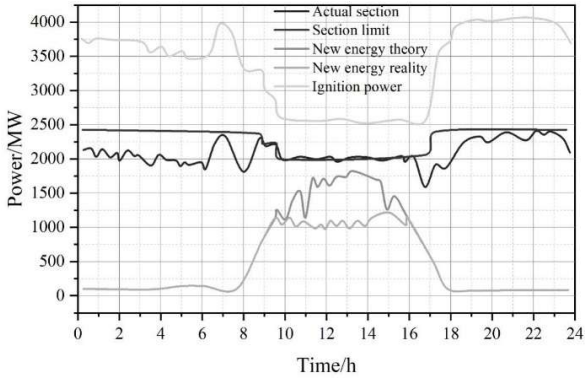

Figure 7: New energy generation curves in power section during the model application

During the 07:00-10:00 time period, the sender section inherently prioritizes the suppression of the output of the units that have not been put into the cutter before the output of the units that have been put into the cutter, resulting in the amount of the cutter associated with this section being automatically adjusted downward, and the amount of the allowable cuts is kept below the section limit during the time of 8:00-10:00, and the power during this period ranges from 1,552 to 2,400 MW, thus realizing the The automatic adjustment of section limit frees up space for new energy generation.

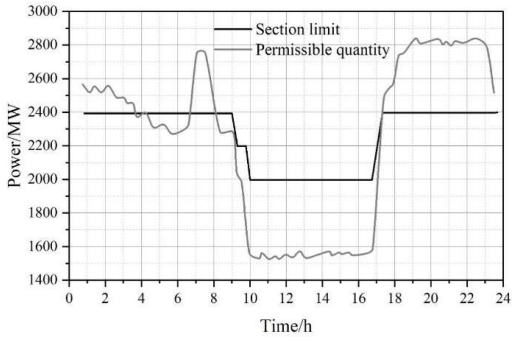

Figure 8: Permissible variation curve

III. C. 2) Effectiveness of corrections

In order to verify the validity of the correction method of new energy ultra-short-term prediction taking into account the operational risk, this paper inputs the new energy ultra-short-term prediction result before correction into the model directly, and obtains the comparison of the power curve of the section before and after correction, as shown in Fig. 9. The new energy output in the section from 09:00 to 09:45 is rising rapidly, and there is no abandonment of power for the time being. Because the new energy ultra-short-term forecast value is on the high side, it is not corrected and directly brought into the model, and the result is: the section limit is downgraded from 2.4 million kW to 1.96 million kW directly at 09:00. And after the revision of the new energy ultra-short-term forecast value, the

section limit is first downgraded from 2.4 million kW to 2.19 million kW at 09:00 hours, and then downgraded to 1.96 million kW at 09:45 hours as the new energy continues to grow. In the case that none of the new energy is limited, the section limit obtained after the correction of the 09:00-09:45 time period is 210-440,000kW larger than that before the correction, which improves the ability to support load centers outside the section and reduces the risk of grid operation, and at the same time, this part of the section space makes the thermal power in the section to be incremented (the incremental amount of the power is shown as the shaded part in the figure), which is more suitable for the The validity of the new energy ultra-short-term forecast correction method is verified.

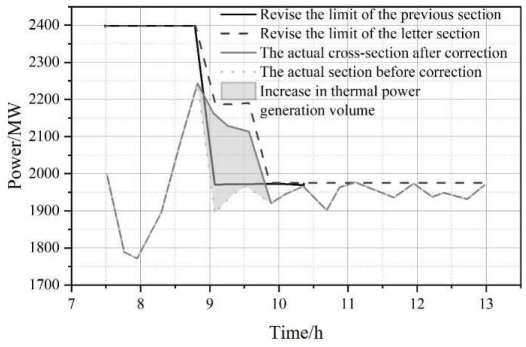

Figure 9: The new energy forecast is revised before and after the delivery of the power

III. D. Assessment of new energy consumption capacity

III. D. 1) Power balance

Based on the new energy consumption-oriented grid planning method proposed in this paper, a certain planning study program for the 2015 power grid in Guangdong Province is analyzed. According to the characteristics of the grid topology and the distribution of loads and power sources in a certain province, the grid of a certain province is divided into five parts: east one, east two, east three, central and west.

This paper utilizes simulation experiments to simulate the power system operation and probabilistic assessment methods to evaluate the new energy consumption capacity, i.e., based on the new energy output sequence simulation technology and power system operation simulation technology to evaluate the new energy consumption capacity considering the main grid trend and section constraints, and to obtain the new energy consumption capacity with a certain level of confidence and the corresponding wind abandonment tolerance level.

III. D. 2) Line utilization and tidal current distribution

Some load shedding exists in all scenarios, but only at very few specific times. For example, on September 23, 2023, when the load peak-to-valley difference was large and the minimum load level was low, wind abandonment and load shedding occurred due to the limitations of the system's regulation capability. Except for that day, no load shedding occurred during the rest of the year, and the scenarios met the province's annual power supply balance needs.

The current and line utilization of each section are shown in Table 1, where 100%, 95%, 90% and 85% indicate the number of periods when the current is greater than 100%, 95%, 90% and 85% of the section capacity, respectively. PI, P2, P3 scheme “East three - East one” section utilization hours increased significantly, divided into 5215h, 5054h, 5125h, section load level is higher, this is related to P1, P2, P3 scheme in the BASE based on the reduction of the capacity of the section, the section capacity of the three schemes are all 2100MW. The utilization hours of “East 3-East 2” section are relatively low, the utilization hours under P1, P2 and P3 schemes are 1958, 1935 and 1465 respectively, but the load level of the section is higher than that of the rest of the sections except “East 3-East 1” section. This is related to the fact that East 1 and 2 are wind power centralized grid-connected areas: the access of wind power increases the current dispersion in the area, and the load level is higher when the wind power output is higher, and lower when the wind power output is lower, which results in a high number of high load hours in the cross-section even with a low utilization rate.

III. D. 3) Distribution of cross-section currents

Further, taking the eastern section of a province under the BASE and P1 schemes as an example (the P2\P3 scheme is similar to P1), the tidal current distribution of this section is analyzed, as shown in Fig. 10, Fig. (a) shows the comparison of the tidal current distribution between the P1 scheme and the BASE scheme, Fig. (b) shows the comparison of the tidal current persistence curves between the P1 scheme and the BASE scheme, and the persistence curve for an eastern section of a province under the BASE scheme is more “full” in Fig. (a). In Fig. (a),

the continuous curve of eastern section of a province under the BASE scheme is more “full”, and there are more periods of high output level when the tidal section is 5000MW, and the probability distribution is between 3% and 5% when the tidal section is 5000MW-8000MW, and the tidal distribution is shifted to the right as a whole.

Table 1: The current situation of the section and the utilization of the line

Case	Section abbreviation	Capacity/ MWA	Maximum trend/MW	Hours	100% Time number /h	95% Time number /h	90%Time number /h	85% Time number /h
BASE case	West	7065	6215	4164	0	0	1	15
	East	10345	10345	3292	30	55	90	185
	Three-one	3020	3020	4216	645	880	1123	1352
	Three-two	3020	3020	2034	40	80	175	280
	One-two	2100	2100	3032	65	100	150	212
Case	Section abbreviation	Capacity/ MWA	Maximum trend/MW	Hours	100% Time number /h	95% Time number /h	90%Time number /h	85% Time number /h
P1 case	West	7065	6484	4398	0	0	2	10
	East	11320	9355	3164	0	0	0	3
	Three-one	2100	2100	5215	2145	2348	2617	2864
	Three-two	3020	2948	1958	0	50	68	150
	One-two	2100	2100	2856	85	135	200	298
Case	Section abbreviation	Capacity/ MWA	Maximum trend/MW	Hours	100% Time number /h	95% Time number /h	90%Time number /h	85% Time number /h
P2 case	West	7065	6484	4315	0	0	2	15
	East	10345	10345	3468	1	1	18	45
	Three-one	2100	2100	5054	2039	2348	2465	2798
	Three-two	3020	2965	1935	0	24	50	123
	One-two	3020	2543	1930	0	0	0	5
Case	Section abbreviation	Capacity/ MWA	Maximum trend/MW	Hours	100% Time number /h	95% Time number /h	90%Time number /h	85% Time number /h
P3 case	West	7065	6484	4385	0	0	2	10
	East	10345	10345	3485	1	3	20	45
	Three-one	2100	2100	5125	2158	2348	2648	2869
	Three-two	4050	2948	1465	0	0	0	2
	One-two	2100	2100	2854	85	140	200	2864

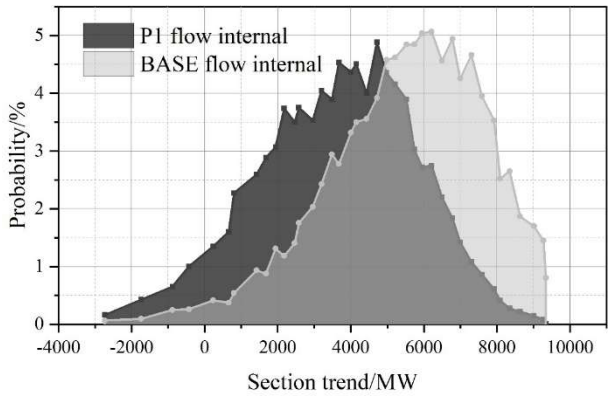

(a)Comparison of power flow distribution between the P1 scheme and the BASE scheme

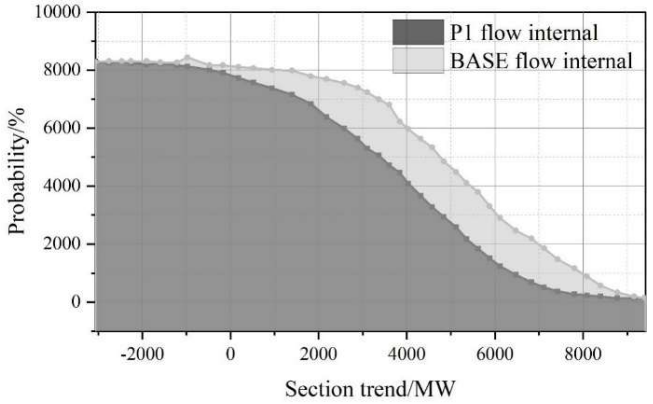

(b)The P1 scheme is compared with the base plan trend

Figure 10: The distribution of cross-sectional tidal currents

III. D. 4) Consumption of new energy sources

Through the operation simulation of the power system, it is found that there is a certain degree of wind curtailment in each scheme, and it is concentrated in the eastern and central regions, and the curtailment results of each planning scheme are shown in Figure 11. Among them, the P2 scenario has the smallest curtailment, with an overall curtailment of 9217.195MW•h, which is significantly smaller than that of other schemes. The P2 scheme strengthens the transmission channel between the "East Zone 1" and the "East Zone 2" in the East Region, so that the "East 2 Zone" with the most wind power can transmit wind power from the East 1 Zone to the Central Zone, and the wind power of the "East Zone 2" can supply power to the Central Zone through the "East Zone 3" and "East Zone 1" at the same time, so the curtailment of wind power is low.

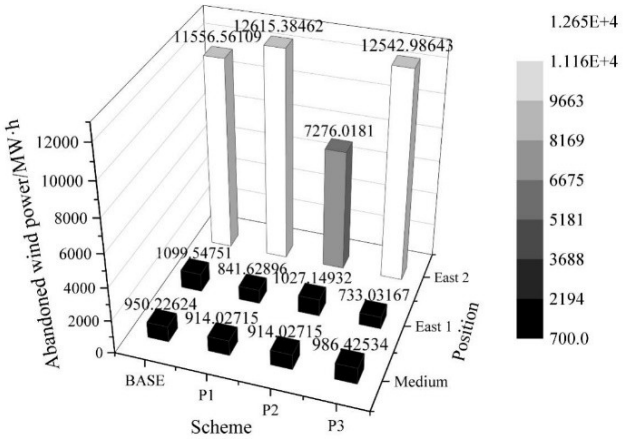

Figure 11: Results of wind power curtailment for each planning scheme

IV. Conclusion

This paper analyzes the calculation idea of new energy consumption capacity, takes into account various constraints, and adopts the calculation method of optimal trend to analyze the new energy consumption capacity. In order to maximize the capacity of new energy power system, the constraints of the objective function and the associated cross section are proposed sequentially. Simulation experiments are used to verify the established new energy consumption capacity assessment model. The load curve of the test area shows that the sequence of load output fluctuates within the range of 1050MW~1610MW during the time period of 0-9000h. Meanwhile, the sequence of wind power output mainly fluctuates between 0.4 and 0.8, and the wind power output decreases to about 0.5 after 8000h. Based on the above basic data, time series production simulation is carried out from January to December to solve the optimization model constructed in this paper. The total annual wind power consumption is 1523076.923MWh, the total wind power abandonment is 120678.733MWh, the wind power abandonment rate is 6.776%, and the utilization hours of wind power generation is 3042.312h. Applying the optimization model to a local grid in a certain area, the new energy output curve and section operation trend in the 07:00-10:00 time period, the new energy output in the sending section continues to increase, and the peak value reaches 2,452MW, which can be seen that the actual operation trend of the sending section is close to the stability limit, and the new energy consumption model that considers the main grid trend and section constraints can substantially Considering the main grid current and section constraints, the new energy consumption model can greatly improve the utilization rate of the section.

References

[1] LI, L., LIU, C., ZHU, H., RAO, Z., & LI, Z. (2023). Absorptive capability evaluation method of renewable energy considering security constraints of power grid. Journal of Electric Power Science and Technology, 38(4), 162-168.

[2] Bilgili, M., Ozbek, A., Sahin, B., & Kahraman, A. (2015). An overview of renewable electric power capacity and progress in new technologies in the world. Renewable and Sustainable Energy Reviews, 49, 323-334.

[3] Impram, S., Nese, S. V., & Oral, B. (2020). Challenges of renewable energy penetration on power system flexibility: A survey. Energy strategy reviews, 31, 100539.

[4] Ibrahim, N. I., Al-Sulaiman, F. A., & Ani, F. N. (2018). Solar absorption systems with integrated absorption energy storage–A review. Renewable and Sustainable Energy Reviews, 82, 1602-1610.

[5] Ang, T. Z., Salem, M., Kamarol, M., Das, H. S., Nazari, M. A., & Prabaharan, N. (2022). A comprehensive study of renewable energy sources: Classifications, challenges and suggestions. Energy strategy reviews, 43, 100939.

[6] Ma, S., Duan, C., Xu, T., Wang, X., Tian, X., & Wang, L. (2020). Cross-regional analysis of new energy consumption capacity. Journal of Beijing Institute of Technology, 29(1), 38-44.
[7] HassanzadehFard, H., & Jalilian, A. (2018). Optimal sizing and location of renewable energy based DG units in distribution systems considering load growth. International Journal of Electrical Power & Energy Systems, 101, 356-370.
[8] Liu, Y., Jiang, Z., Sun, Y., Yang, X., Wang, X., & Zhang, D. (2024). Research on the calculation method of the reasonable utilization rate of renewable energy considering generation–grid–load–storage coordinated planning. Frontiers in Energy Research, 11, 1343967.
[9] Huang, S., Wang, J., Li, Z., Li, S., & Wang, C. (2021, March). Research on New Energy Consumption Capacity Based on Grid Aggregation Model. In IOP Conference Series: Earth and Environmental Science (Vol. 714, No. 4, p. 042071). IOP Publishing.
[10] Meng, X., Zhang, S., Liu, H., & Zhou, S. (2024). A method of energy storage capacity planning to achieve the target consumption of renewable energy. Journal of Energy Storage, 97, 112993.
[11] Huang, K., Jiao, B., Zhang, S., Liu, H., & Sun, L. (2022, December). Calculation method of consumption capacity of photovoltaic distribution network based on Time Series Production Simulation. In Journal of Physics: Conference Series (Vol. 2401, No. 1, p. 012060). IOP Publishing.
[12] Shi, Q., Yang, P., Tang, B., Lin, J., Yu, G., & Muyeen, S. M. (2023). Active distribution network type identification method of high proportion new energy power system based on source-load matching. International journal of electrical power & energy systems, 153, 109411.
[13] Gils, H. C., Scholz, Y., Pregger, T., de Tena, D. L., & Heide, D. (2017). Integrated modelling of variable renewable energy-based power supply in Europe. Energy, 123, 173-188.
[14] Yang, C., Sun, Y., Zou, Y., Zheng, F., Liu, S., Zhao, B., ... & Cui, H. (2023). Optimal power flow in distribution network: A review on problem formulation and optimization methods. Energies, 16(16), 5974.
[15] Dall'Anese, E., Baker, K., & Summers, T. (2017). Chance-constrained AC optimal power flow for distribution systems with renewables. IEEE Transactions on Power Systems, 32(5), 3427-3438.
[16] Li, Y., He, S., Li, Y., Ding, Q., & Zeng, Z. (2023). Renewable energy absorption oriented many-objective probabilistic optimal power flow. IEEE Transactions on Network Science and Engineering.
[17] Yang Liu,Min Huang,Yujing Zhang,Lu Zhang,Wenbin Liu,Haidong Yu... & Lisheng Li. (2025). Coordinated Optimization Method of Electric Buses and Voltage Source Converters for Improving the Absorption Capacity of New Energy Sources and Loads in Distribution Networks.Energies,18(4),832-832.
[18] You Lei,Ma Hui & Kumar Saha Tapan. (2023). A CVaR-constrained optimal power flow model for wind integrated power systems considering Transmission-side flexibility. International Journal of Electrical Power and Energy Systems,150,
[19] Yong Li,Hua Wang,Xianbin Huang,Juanyang Hao,Wenting Lei & Quanlin Wang. (2025). Short-term power load forecasting in distribution networks considering human comfort level. Frontiers in Energy Research,13,1514755-1514755.